Journal of Pharmaceutical and Biomedical Analysis 194 (2021) 113805

Contents lists available at ScienceDirect

Journal of Pharmaceutical and Biomedical Analysis

journal homepage: www.elsevier.com/locate/jpba

Laser induced breakdown spectroscopy with machine learning reveals lithium-induced electrolyte imbalance in the kidneys

Irfan Ahmed[a,b], Muhammad Shehzad Khan[a], Santosh Paidi[c], Zhenhui Liu[c], Chi Zhang[c], Yuanchao Liu[a], Gulsher Ali Baloch[b], Alan W.L. Law[a], Yanpeng Zhang[d], Ishan Barman[c,e,f,*], Condon Lau[a,*]

[a] Department of Physics, City University of Hong Kong, Hong Kong SAR, China
[b] Department of Electrical Engineering, Sukkur IBA University, Sukkur, Pakistan
[c] Department of Mechanical Engineering, Johns Hopkins University, Baltimore, USA
[d] Key Laboratory for Physical Electronics and Devices of the Ministry of Education & Shaanxi Key Lab of Information Photonic Technique, Xi'an Jiaotong University, Xi'an, China
[e] Department of Oncology, Johns Hopkins University School of Medicine, Baltimore, MD, USA
[f] Department of Radiology & Radiological Science, Johns Hopkins University School of Medicine, Baltimore, MD, USA

ARTICLE INFO

Article history:
Received 5 October 2020
Received in revised form
24 November 2020
Accepted 25 November 2020
Available online 5 December 2020

Keywords:
Lithium
Renal
Kidney
Electrolytes
Spectroscopy
Machine learning

ABSTRACT

Lithium is a major psychiatric medication, especially as long-term maintenance medication for Bipolar Disorder. Despite its effectiveness, lithium has side-effects, such as on renal function. In this study, lithium was administered to adult rats. This animal model of renal function was validated by measuring blood lithium, urea nitrogen (BUN), and thyroxine (T_4) using inductively-coupled plasma mass spectrometry and enzyme-linked immunosorbent assay. The kidneys were analyzed by laser induced breakdown spectroscopy (LIBS) with 1064 nm ablation and 300–900 nm detection. Principal components analysis (PCA), radial visualization, and random forest classification were performed on the LIBS spectra for multi-element prediction and classification. Lithium at 0.34 mmol/L was detected in the blood of lithium treated subjects only. BUN was increased (6.6 vs. 5.3 mmol/L) and T_4 decreased (58.12 vs. 51.4 mmol/L) in the blood of lithium subjects compared with controls, indicating renal abnormalities. LIBS detected lithium at 2.3 mmol/kg in the kidneys of lithium subjects only. Calcium was also observed to be reduced in lithium subjects, compared with controls. Subsequent PCA observed a change in the balance of sodium and potassium in the kidneys. These are key electrolytes in the body. Importantly, partial least squares regression showed that standard clinical measurements, such as the blood tests, can be used to predict kidney electrolyte measurements, which typically cannot be performed in humans. Overall, lithium accumulates in the kidneys and adversely affects renal function. The effects are likely related to electrolyte imbalance. LIBS with machine learning analysis has potential to improve clinical management of renal side-effects in patients on lithium medication.

1. Introduction

Lithium's toxic effects had limited its clinical use until appropriate serum monitoring became readily available. Since then, lithium therapy is effectively used for treating bipolar disorder and other mental illnesses with proper monitoring of lithium serum levels [1]. Lithium has a low therapeutic index and is freely filtered, but over 60 percent is then re-absorbed by the proximal tubules. In general, many patients on chronic lithium therapy experience at least one episode of toxicity during treatment [2]. Further, lithium is associated with thyroid, overall endocrine dysfunction, adverse effects on the kidneys, and cardio-toxicity [3–6]. In particular, chronic lithium ingestion in patients has been associated with several different forms of renal injury [7]. Nephrogenic diabetes insipidus is the most common renal side effect of lithium therapy [8,9]. Unfortunately, relatively little is known about the characterization of lithium in the kidneys, particularly potential glomerular toxicity of lithium and nephrotic syndrome in both infants and adults.

One important aspect of renal function that requires investigation is the impact of lithium on key electrolytes, such as sodium, potassium, calcium, and magnesium. Further, electrolyte balance

* Corresponding authors.
E-mail addresses: ibarman@jhu.edu (I. Barman), condon.lau@cityu.edu.hk (C. Lau).

https://doi.org/10.1016/j.jpba.2020.113805
0731-7085/

in the kidneys needs to be related to systemic measures of renal function, such as blood urea nitrogen (BUN) levels. To study these electrolytes and their balance in the presence of lithium, laser induced breakdown spectroscopy (LIBS) is a promising analytical method. LIBS employs a pulsed to ablate the sample and record the resulting optical emission, which is characteristic of the elements in the sample [10–13]. LIBS has consistently demonstrated the capability to rapidly detect, biochemically characterize and analyze, and/or accurately identify various biological, biomedical or clinical samples [14]. LIBS has also been used to investigate electrolytes in plasma [15,16] and is very sensitive to the light weight lithium atom [17,18]. It has previously been applied to analyze the kidneys [19,20].

Traditionally, LIBS data was analyzed by matching observed emission lines with the corresponding element. Further quantitative analysis was often performed by calibrating the height of a line with the concentration of the element in the sample. In recent years, multivariate chemometrics has been combined with LIBS to further analyze the data [21,22]. Methods such as partial least-squares regression, artificial neural network, support vector machine, random forest regression, multi-linear regression, principal component regression, and standard addition have been widely applied to LIBS data in predicting the concentration of elements and classification [15,16,23–27].

Previously, we detected trace lithium in the breast milk of mothers (rat) administered lithium [17] and in the thyroid of adults (rat) [18]. Here, we study the impact of lithium on renal function and kidney electrolyte balance. We employ inductively coupled mass spectroscopy (ICP-MS) and enzyme-linked immunosorbent assay (ELISA) to measure blood lithium, urea nitrogen, and thyroxine (T_4) levels. These are systemic measures of renal function. We develop LIBS with machine learning analysis, specifically principal components analysis (PCA), radial visualization (RadViz), and random forest classifier, to study kidney electrolyte balance and to link systemic and in situ kidney measures of renal function. The results show systemic lithium-induced renal dysfunction likely related to kidney electrolyte imbalance. Further, a classifier is built that predicts kidney electrolyte levels, which cannot be easily measured in vivo, using the minimally invasive blood test measures.

2. Methods

2.1. Animal subject

Male Sprague Dawley (SD) rats (N = 10, 175–200 g) of 6 weeks age were employed for the study. The AAALAC accredited Laboratory Animal Unit of the University of Hong Kong provided the subjects. Animal research ethics committees of the City University of Hong Kong, the University of Hong Kong, and the Department of Health of the Hong Kong Special Administrative Region approved the study. Each subject was housed individually in a cage at a temperature of 25 °C and humidity of 60–70% in the Laboratory Animal Research Unit of the City University of Hong Kong. All subjects were housed in 12/12 h light/dark cycles and had access to regular chow food and drinking water.

2.2. Lithium administration

Lithium carbonate (Li_2CO_3) was purchased from Sigma Aldrich (USA). For the lithium treatment group (N = 5), 2000 mg of Li_2CO_3 per kilogram of body weight was administered via gavage twice per day for five days. Refer to reference [17] for details on preparing the Li_2CO_3 solution. The control group was similarly administered distilled water.

2.3. Sample preparation

On 6th day of lithium administration, subjects were weighed first and then euthanized by 1 mL/kg body weight of 20% Dorminal administered via intraperitoneal injection. Later, the subjects were dissected to extract the blood from their hearts using a 1 mL syringe with 25 gauge needle. Two ml of blood was collected in two 1 mL tubes, with 1 mL for measuring BUN and T_4 hormones and 1 mL for measuring serum lithium concentration. For T_4 and BUN, ELISA was applied. ELISA sandwich enzyme immunoassay-based kits were purchased from BioMedical Assay for T4 and BUN. T4 and BUN levels were measured for control and lithium groups. The blood lithium concentration was measured using ICP-MS. Following the blood extraction, the kidneys were surgically extracted. The excised kidneys were immersed in saline to remove blood. Freeze-drying was subsequently performed as per the protocol defined in [17] before LIBS data acquisition. After LIBS data acquisition and analysis, two kidney samples of 1 gm each were prepared from 5 controls and 5 lithium subjects for quantification of elements suggested by the analysis.

2.4. Spectroscopic experiments

Fig. 1 shows the setup of LIBS along with the workflow. The 1064 nm pulsed laser (CFR200, Quantel) emitted 8 ns, 200 mJ pulses focused to a 40 μm spot on the sample. The optical emission from the sample was collected by a six-channel fiber (2000 μm diameter) bundle, positioned 35 mm from the focus and at 45° from the laser beam. The fibers relayed light to six spectrometers spanning 200–900 nm with 0.1 nm resolution (MX2500+, Ocean Optics). The spectrometer was triggered to acquire 2 μs after laser firing and with 1 ms acquisition. Apart from sample preparation and LIBS experimentation, wavelength calibration has been adapted from the previously published articles [17,28].

For quantification of serum lithium, ICP-MS (Perkin Elmer DRC II) was employed as per the protocol of AOAC INTERNATIONAL [29]. One ml of blood was centrifuged at 2500 rpm and the serum extracted. Approximately 0.5 g was weighed in a digestion vessel with nitric acid and hydrogen peroxide added. The resulting solution underwent microwave digestion (Milestone ETHOS) for 9 min. at 200 °C. The digested solution was made up to 12.5 mL with Milli-Q water. Calcium, sodium, lithium and potassium were analyzed with corresponding reference solutions for calibration.

2.5. Data acquisition and processing

Measurements for LIBS were obtained in standard air atmosphere. Prior to LIBS, samples were placed at pre-marked positions on the slide to facilitate rapid sample positioning. At the time of acquisition, the slide was placed on the sample holder with the sample at the laser focus. Five sites on each kidney were ablated by firing two laser shots at each. Emission spectra for the shots were recorded separately for left (10 shots) and right (10 shots) kidneys for each subject. A PC synchronized the setup and processed spectral data acquired by the spectrometers, producing a graphical presentation of spectral intensity against the corresponding wavelength. The raw data from the LIBS spectrometer was imported into OriginLab software for baseline correction. For baseline correction, every time a baseline was acquired prior to measurement of each subject and was subtracted from each spectrum followed by normalization of the intensity of each spectrum. Normalization was to the 656.2 nm hydrogen line as hydrogen is a structural element not likely to be affected by lithium treatment. Next, the normalized spectra from the twenty laser pulses fired at both kidneys (left and

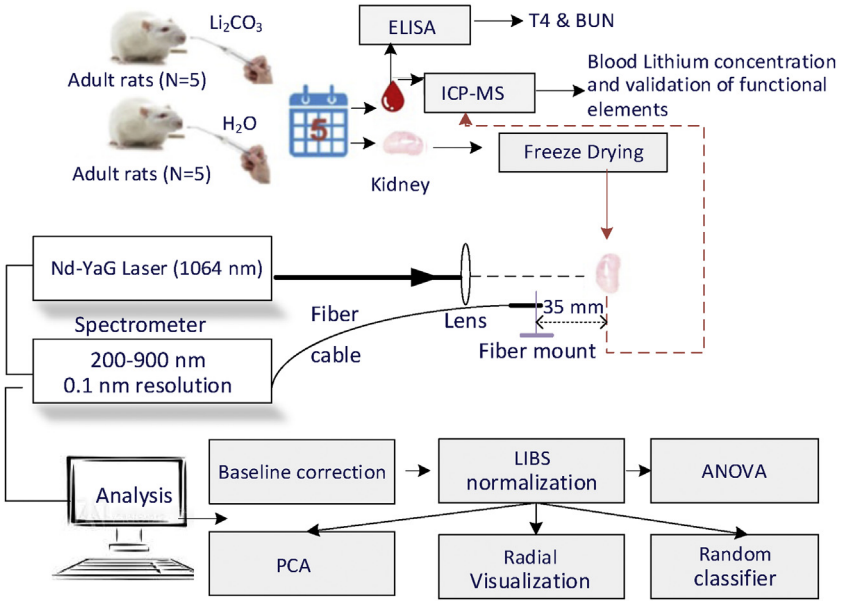

Fig. 1. Workflow of the study.

Table 1
Monitored blood data analysis and pre- and post-experimental weights of control (C) and lithium (Li) treated subjects. * represents $p < 0.05$ and LOD is limit of detection.

S.NO	BUN (mmol/L)		T_4 (nmol/L)		BLi (mmol/L)		Pre-experiment Weight (g)		Post-experiment Weight (g)	
	C	Li	C	Li	C	Li	C	Li	C	Li
1	5.5	6.2	53.5	28.8	<LOD	0.42	175	186	212	195
2	5.4	6.1	63.7	57.3	<LOD	0.34	179	190	217	209
3	5.5	7.9	61.1	56.6	<LOD	0.30	189	190	213	230
4	5.1	7.2	51.7	53.2	<LOD	0.35	191	200	211	212
5	5.2	5.6	60.6	61.3	<LOD	0.27	188	192	214	217
Mean	5.3	6.6	58.12	51.4	<LOD	0.34	184.4	191.6	213.4	212.6
STD	0.2 *	0.9	5.2	12.9 *		0.05	6.9	5.2	2.3	12.7

right) of each subject were averaged to obtain the mean spectrum along with standard deviation.

2.6. Statistical analysis and machine learning

Statistical analysis of the spectra obtained from the kidneys was performed using one-way ANOVA across the elements and subject groups. A post hoc analysis using a two-tail *t*-test of equal variance was performed. A p-value threshold of 0.05 was considered statistically significant. The spectral dataset of LIBS was individually subjected to PCA using Python to obtain principal components (PCs) scores and loadings. Radial visualization maps were plotted using the RadViz tool from the Orange data mining toolbox. Here, we employed the scores of select PCs obtained from subjecting the individual spectral dataset of LIBS to PCA, we also calculated the confusion matrix based on PCA analysis. In the radial visualization plot, the scores of a spectrum determine the position of the corresponding data point relative to the PC pivots. Later, random classifier plotted against the spectral wavelength was employed to suggest the classifier predictor followed by out of bag classification error obtained from random forest. Based on Partial least squares (PLS) regression, we predicted internal LIBS measurements of kidney elements from BUN, T4, BLI and pre and post experimental weight of the subjects. Note that the in-situ kidney measurements cannot be directly measured from humans while the blood test and body weight measurements can be obtained with minimal invasiveness. Therefore, this predictor has potential clinical value.

3. Results and discussion

Table 1 presents BUN, blood T_4, and blood lithium concentration measured from lithium-treated subjects and control subjects along with their means and standard deviations (STD). BUN and T_4 are measured using ELISA while blood lithium is measured using ICP-MS. We also measured the pre- and post-experiment weight of the subjects. It is interesting that BUN is significantly increased ($p < 0.0.5$) with the intake of lithium while blood lithium is not surprisingly increased ($p < 0.05$). We also see some reduced trend of T_4 hormones in lithium subjects when compared with the control.

Fig. 2 shows the LIBS spectrum obtained from kidneys (left and right) of a control subject. Fig. 2(a) shows the whole spectrum from 300 to 900 nm. There were several prominent emission lines showing the spectral signature of functional electrolyte elements. The sub-panels, Figs. 3(b-e), show the spectrum expanded about different wavelength ranges. Calcium lines were observed at 393.4, 396.9 and 422.7 nm. Sodium lines were observed at 589.0 and 589.5 nm. A prominent hydrogen line was observed at 656.2 nm. Potassium lines were observed at 766.4 and 769.9 nm. Amongst the key electrolytes, Na lines had the highest intensity, followed by K in the control group. The un-normalized intensity (mean ± standard deviation) for each emission line (Ca, Na, H, and K) is averaged over the 20 shots for each subject. The un-normalized intensity measured for Ca, Na, H, and K (averaged across lines from the same element) from control subjects were 366.4 ± 221.2, 13303 ± 1996, 2442 ± 1092, and 10303 ± 3514 a.u., respectively. It should be noted

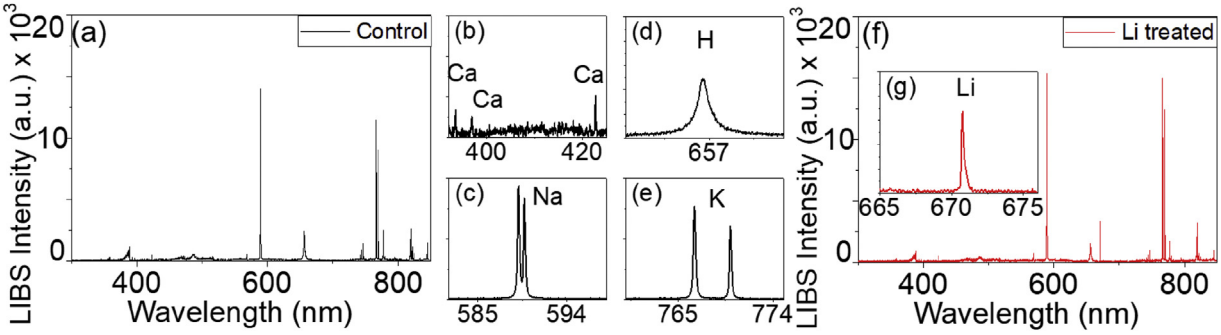

Fig. 2. (a) Averaged LIBS spectrum from the 20 shots fired at the left and right kidneys of a control subject. (b) Calcium (Ca) was observed at 393.4, 396.9 and 422.7 nm. (c) Sodium (Na) lines were observed at 589.0 and 589.5 nm. (d) The hydrogen (H) line was observed at 656.2 nm. (e) Potassium (K) lines were observed at 766.4 and 769.9 nm. (f) Averaged LIBS spectrum from the 20 shots fired at the left and right kidneys of a lithium-treated subject. (g) Lithium (Li) line observed from lithium-treated subject at 670.7 nm.

Table 2
Confusion matrix using PCA bases on 50/ 50 train test split.

n = 100	Predicted Control	Predicted Lithium	Total
Actual Control	39	11	50
Actual Lithium	10	40	50

that no lithium emission line was observed in any control subject. Fig. 2(f) shows the whole spectrum from 300 to 900 nm from a lithium subject. In lithium-treated subjects, the lithium emission line is observed at 670.7 with an intensity of 3363 ± 668 a.u, shown in Fig. 2(g). The averaged measurements for Ca, Na, H, and K from lithium subjects are 331 ± 48, 14440.5 ± 1012, 1475 ± 94 and 13754 ± 1156 a.u., respectively.

Fig. 3 shows the bar plots with the mean and standard error of LIBS emission intensities of Ca, Na, Li and K from the kidneys of control and 5 days lithium-treated subjects. LIBS intensities have been normalized by the 656.2 nm hydrogen line intensity. From LIBS measurements, the changes in intensities of lithium and calcium were found to be statistically significant ($p < 0.05$) with the intake of lithium. The accumulation of lithium in kidneys was quantified using ICP-MS, which was observed to be 2.3 mmol/kg for treated subjects and below limit of detection for controls. Further, the calcium was quantified at 5 mmol/kg in control and 4.5 mmol/kg in lithium-treated subjects. The quantification of sodium and potassium shows a consistent trend through ICP-MS measurements. The sodium and potassium were quantified as 450 and 495 mmol/kg, respectively, in control and 144.25 mmol/kg and 170 mmol/kg in lithium-treated subjects. The Na and K ratio was increased from 0.95 ± 15 to 1.10 ± 0.10 with the accumulation of lithium in kidneys when measured with LIBS. The ICP-MS also demonstrated a similar trend from 2.8 to 2.9 mmol/kg.

In Fig. 4(a), PCA scores have been derived from 200 hydrogen normalized LIBS spectra (with background subtraction) of kidney samples from control and lithium-treated subjects. Each point in the scatter plot (score plot) represents one spectrum. From the visual inspection in Fig. 4(a), few of the control and lithium-treated spectra are clearly classified. However, Fig, 4(b) shows more visual difference between the control and lithium treated group. To verify the robustness of the PCA classifier, we calculated the confusion matrix based on 1000 iterations and 50/50 train test split. Table 2 presents the confusion matrix from PCA spectral analysis. This indicates that the kidney LIBS spectra of control and lithium-treated subjects are significantly different.

In Fig. 4(c), we present whole spectrum loadings. The three PCs suggested overall variance of 99%. Fig. 4(c) displays the first three PC loadings derived from LIBS and covers 99% (98%, 0.7% and 0.3%) of the variance. It can be seen that sodium and potassium are major classifiers other than lithium. In PC2 and PC3, it can be seen that

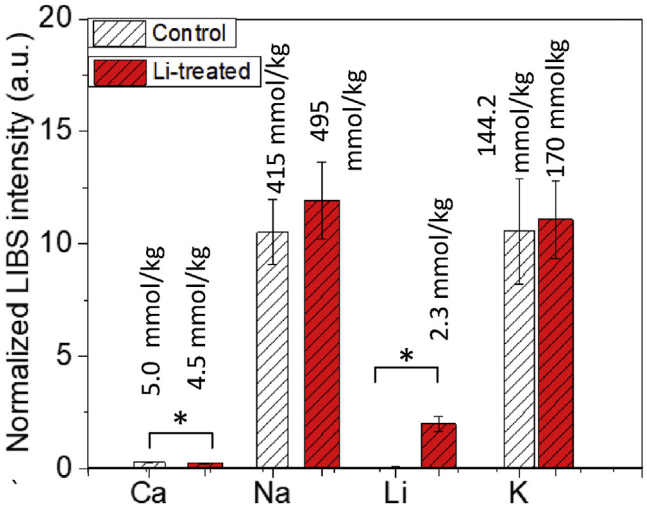

Fig. 3. Bar plots showing the mean and standard error of LIBS emission intensities for Ca, Na, Li, and K from the kidneys of control (N = 5) and 5 days lithium-treated subjects (N = 5). Statistical analysis between groups was performed with one-way ANOVA. A post hoc analysis using a two-tail *t*-test of equal variance was performed with a p-value threshold of 0.05 considered statistically significant. For quantification of calcium, sodium, lithium and potassium, ICP-MS was employed. The samples, after LIBS measurement, were digested using HNO_3 and H_2O_2 and ICP-MS was performed as per the AOAC protocol. * indicates $p < 0.05$.

sodium has positive loading across the PCs. This means that sodium is considerably different between the two subject groups and this is supported by mean emission intensities in Fig. 3. In contrast, potassium is positive in PC1, near 0 in PC2, and negative in PC3. This means that potassium is less different between the groups and this concurs with Fig. 3. This suggests that lithium causes Na-K imbalance in the kidneys. To emphasize these differences better, we used radial visualization plots that map the scores of multiple PCs onto a two-dimensional space for the purpose of clustering. Fig. 4(d) shows the radial visualization plot constructed through PCs from the total set of spectra. Fig. 4(d) suggests that clusters classification visual perspective is revolve around PC2 and PC3. The bar plot for control and lithium subjects in Fig. 4(e) obtained from PC3 scores shows statistically significant difference between LIBS spectra from control and lithium groups. As Na and K lines have opposite signs in PC3 (see panel c), this quantifies the Na-K imbalance in the kidneys.

Table 2 displays the confusion matrix using PCA bases 50/50 (control/lithium) train test split. The actual correct control spectra prediction was 39, whereas 40 lithium spectra were correctly predicted. There were 10 incorrect control predictions which were lithium and 11 lithium predictions which were control.

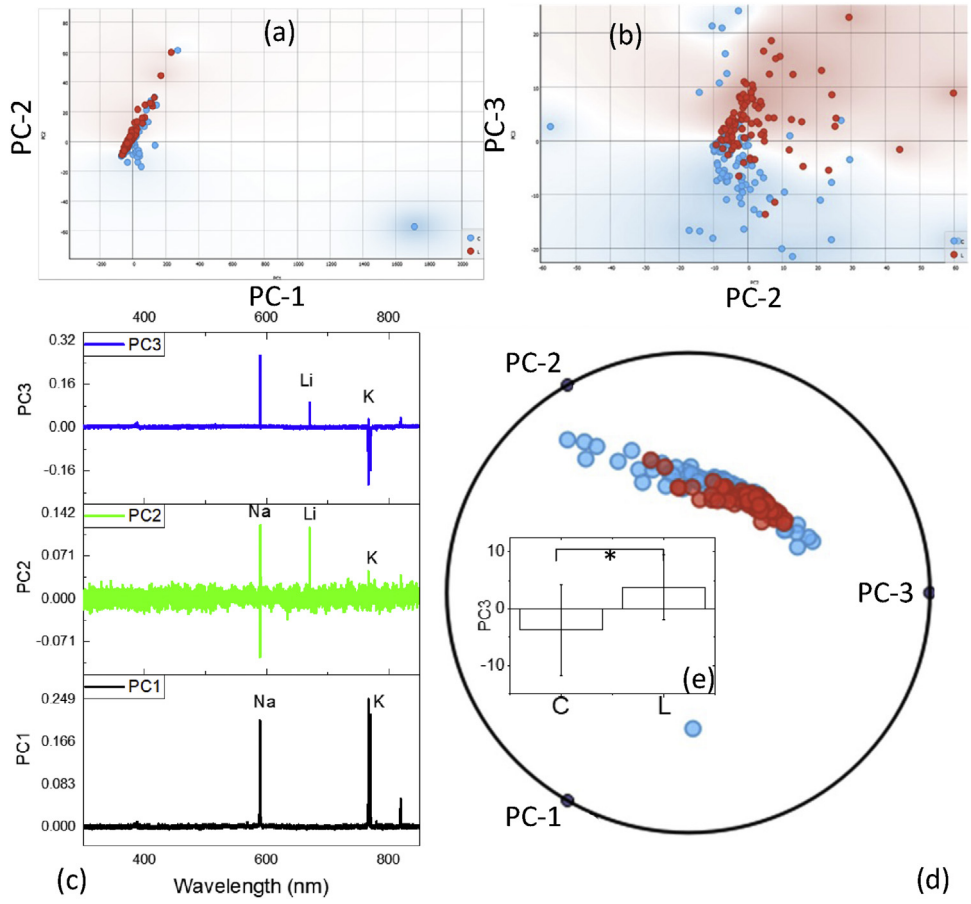

Fig. 4. (a) PCA score plots (PC1 vs PC2) and (b) PCA score plots (PC2 vs PC3) derived from kidney LIBS spectra of control (in blue) and lithium treated subjects (in red). (c) shows the corresponding PC loadings (PC1-PC3) plotted against the spectral wavelength (nm). (d) Visualization of spectroscopic differences illustrated by cluster of control (in blue) and lithium subject (in red). (e) Bar plot for control and lithium subjects obtained from PC3 scores.

A random forest prediction algorithm was trained against the LIBS spectral data, with the predictors based upon the characteristic wavelengths (200–900 nm). Importantly, the random forest approach identified lithium as important variables or predictor responsible for classification among the subjects as suggested by Fig, 5(a). To measure the prediction error, out of bag (OOB) classification error was calculated against the number of grown trees. The OOB error is reduced with increasing number of grown trees suggesting promising validation of random classifier and accuracy of the lithium predictor based on the LIBS measurement.

Fig. 6(a–c) are the predicted sodium, lithium, and potassium lines LIBS intensities. PLS regression was employed to predict the LIBS measurements from the kidneys using blood (BUN, T_4, Li) and body weight measurements. Fig. 6(d) is the similarly predicted Na/K ratio. Note that the kidney measurements cannot be typically performed in humans, but the blood and body weight measurements can be performed with minimal invasiveness. The predicted R^2 of lithium and mean square error are 0.97 and 0.01, respectively, suggesting that kidney lithium can be very accurately predicted. This agrees with the random forest classification in Fig. 5. Also, kidney sodium is predicted with accuracy (R^2 0.75 and MSE 0.67). The ability to predict kidney lithium can be used to track kidney lithium concentration during lithium therapy of bipolar disorder patients using standard clinical measures (ie. blood tests). Overall, lithium accumulates in the kidneys and adversely affects renal function. The effects are likely related to electrolyte imbalance. In the last five decades, there has been limited knowledge about renal adverse effects, which has led clinicians to either avoid or prematurely discontinue lithium therapy because of the perceived risk of a negative renal outcome [30]. Therefore, these predictions can likely improve the monitoring of lithium side-effects and help to optimize the efficacy and safety of lithium therapy.

4. Summary

In this study, lithium was administered to adult rats to investigate the electrolytic balance in kidneys by laser induced breakdown spectroscopy. Lithium was detected in the blood of lithium treated subjects only. BUN was increased in the blood of lithium subjects compared with controls, indicating renal abnormalities. LIBS detected lithium in the kidneys of lithium subjects only. Calcium was also observed to be reduced in lithium subjects, compared with controls. We developed LIBS with machine learning analysis to study kidney electrolyte balance and to link systemic and in situ kidney measures of renal function. PCA observed a change in the balance of sodium and potassium in the kidneys. A partial least squares classifier was built that predicted kidney electrolyte levels, which cannot be easily measured in vivo, using the minimally invasive blood test measures. Overall, lithium accumulates in the kidneys and adversely affects renal function. The effects are likely related to electrolyte imbalance. LIBS with machine learning analysis has potential to improve clinical management of renal side-effects in patients on lithium medication.

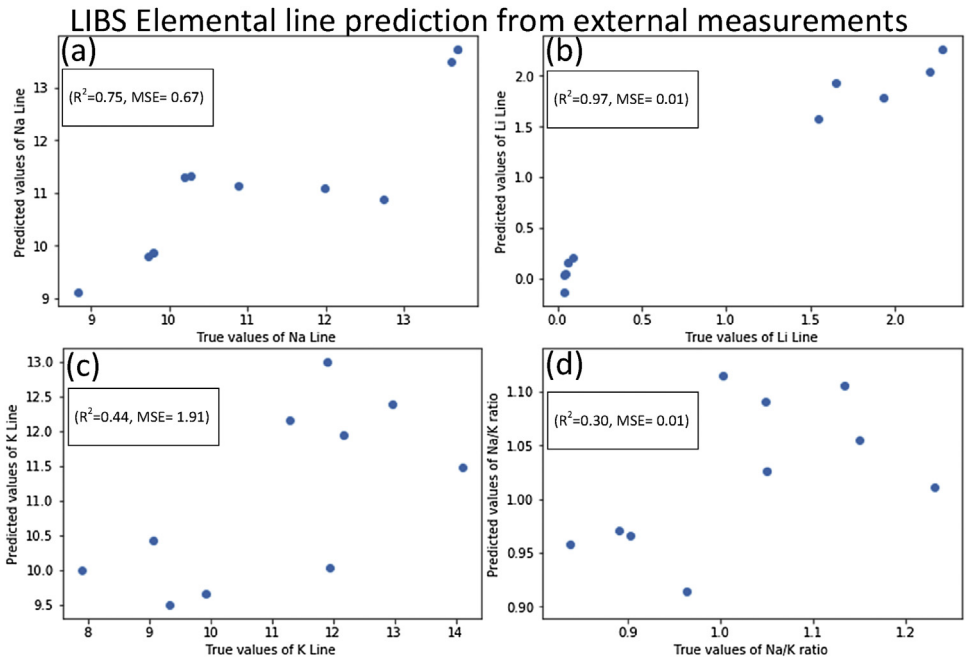

Fig. 6. (a), (b) and (c) Predicted kidney sodium, lithium, and potassium lines LIBS intensity (normalized to H line). (d) Predicted Na/K intensity ratio. This prediction is based on partial least square regression by training the external measurements (BUN, blood lithium, blood T_4, pre and post experimental weights) to predict the LIBS measurements. Note that the former can be measured with minimal invasiveness in clinical practice, while the latter typically cannot be measured in humans.

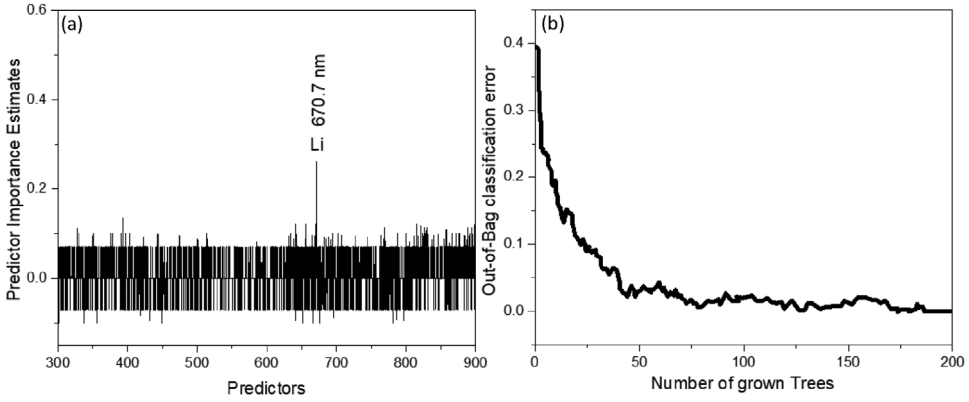

Fig. 5. (a). shows the predictors from random classifier plotted against the spectral wavelength. (b) shows the out of bag classification error obtained from random forest.

Funding sources

This research was supported by start-up funding from the City University of Hong Kong (project numbers 7200414 and 9610338).

Author Statement

IA, SHM and AWLL performed the experiments, SKP, ZL, CZ, YL, GAB helped in analyzing the data. IA, IB, YZ, and CL contributed in writing the manuscript. IA, CL and IB supervised the whole work. All authors have given approval to the final version of the manuscript.

Declaration of Competing Interest

The authors declare that they have no known competing financial interests or personal relationships that could have appeared to influence the work reported in this paper.

References

[1] M. Jeanmarie Perrone, MDFACMTPia Chatterjee MD, Lithium poisoning, UpToDate, 2019 https://www.uptodate.com/contents/lithium-poisoning?topicRef=2358&source=see_link.
[2] A. Amdisen, A. Amdisen, Clinical features and management of lithium poisoning, Med. Toxicol. Adverse Drug Exp. 3 (1988), 18–32http://www.ncbi.nlm.nih.gov/pubmed/3285125(accessed July 5, 2019).
[3] B. Shine, R.F. McKnight, L. Leaver, J.R. Geddes, Long-term effects of lithium on renal, thyroid, and parathyroid function: a retrospective analysis of laboratory data, Lancet. 386 (2015) 461–468, http://dx.doi.org/10.1016/S0140-6736(14)61842-0.
[4] E.G. Smith, Long-term effects of lithium on renal function, Lancet. 386 (2015) 1943, http://dx.doi.org/10.1016/S0140-6736(15)00832-6.
[5] S. Rej, K. Shulman, N. Herrmann, Long-term effects of lithium on renal function, Lancet. 386 (2015) 1943–1944, http://dx.doi.org/10.1016/S0140-6736(15)00834-X.
[6] W.S. Waring, Delayed cardiotoxicity in chronic Lithium poisoning: discrepancy between serum Lithium concentrations and clinical status, Basic Clin. Pharmacol. Toxicol. 100 (2007) 353–355, http://dx.doi.org/10.1111/j.1742-7843.2007.00054.x.
[7] M. Gitlin, M. Gitlin, Lithium and the kidney: an updated review, Drug Saf. 20 (1999) 231–243, http://dx.doi.org/10.2165/00002018-199920030-00004.
[8] R.F. McKnight, M. Adida, K. Budge, S. Stockton, G.M. Goodwin, J.R. Geddes, Lithium toxicity profile: a systematic review and meta-analysis, Lancet

(London, England). 379 (2012) 721–728, http://dx.doi.org/10.1016/S0140-6736(11)61516-X.
[9] F. Trepiccione, B.M. Christensen, Lithium-induced nephrogenic diabetes insipidus: new clinical and experimental findings, J. Nephrol. 23 (Suppl 16) (2010) S43-8 (accessed July 5, 2019) http://www.ncbi.nlm.nih.gov/pubmed/21170888.
[10] G. Yang, Q. Lin, Y. Ding, D. Tian, Y. Duan, Laser Induced Breakdown Spectroscopy Based on Single Beam Splitting and Geometric Configuration for Effective Signal Enhancement, Sci. Rep. 5 (2015) 1–11, http://dx.doi.org/10.1038/srep07625.
[11] S.K. Hussain Shah, J. Iqbal, P. Ahmad, M.U. Khandaker, S. Haq, M. Naeem, Laser induced breakdown spectroscopy methods and applications: a comprehensive revie, Radiat. Phys. Chem. 170 (2020), 108666, http://dx.doi.org/10.1016/j.radphyschem.2019.108666.
[12] P.B. Dixon, D.W. Hahn, Feasibility of detection and identification of individual bioaerosols using laser-induced breakdown spectroscopy, Anal. Chem. 77 (2005) 631–638, http://dx.doi.org/10.1021/ac048838i.
[13] R.S. Harmon, R.E. Russo, R.R. Hark, Applications of laser-induced breakdown spectroscopy for geochemical and environmental analysis: a comprehensive review, Spectrochim. Acta - Part B At. Spectrosc. 87 (2013) 11–26, http://dx.doi.org/10.1016/j.sab.2013.05.017.
[14] S.J. Rehse, H. Salimnia, A.W. Miziolek, Laser-induced breakdown spectroscopy (LIBS): an overview of recent progress and future potential for biomedical applications, J. Med, Eng. Technol. 36 (2012) 77–89, http://dx.doi.org/10.3109/03091902.2011.645946.
[15] A.N. Williams, S. Phongikaroon, Laser-induced breakdown spectroscopy (LIBS) in a novel molten salt aerosol system, Appl. Spectrosc. 71 (2017) 744–749, http://dx.doi.org/10.1177/0003702816648965.
[16] X. Chen, X. Li, S. Yang, X. Yu, A. Liu, Discrimination of lymphoma using laser-induced breakdown spectroscopy conducted on whole blood samples, Biomed. Opt. Express 9 (2018) 1057, http://dx.doi.org/10.1364/boe.9.001057.
[17] I. Ahmed, F.A.M. Manno, S.H.C. Manno, Y. Liu, Y. Zhang, C. Lau, Detection of lithium in breast milk and in situ elemental analysis of the mammary gland, Biomed. Opt. Express 9 (2018), http://dx.doi.org/10.1364/BOE.9.004184.
[18] I. Ahmed, J. Yang, A.W.L. Law, F.A.M. Manno, R. Ahmed, Y. Zhang, C. Lau, Rapid and in situ optical detection of trace lithium in tissues, Biomed. Opt. Express 9 (2018), http://dx.doi.org/10.1364/BOE.9.004459.
[19] W. Meyer, R. Engelhardt, P. Hering, Laser induced breakdown spectroscopy (LIBS) of kidney stones, in: Laser Lithotr, Springer, Berlin Heidelberg, 1988, pp. 25–30, http://dx.doi.org/10.1007/978-3-642-73864-7_3.
[20] B.G. Oztoprak, J. Gonzalez, J. Yoo, T. Gulecen, N. Mutlu, R.E. Russo, O. Gundogdu, A. Demir, Analysis and classification of heterogeneous kidney stones using laser-induced breakdown spectroscopy (LIBS), Appl. Spectrosc. 66 (2012) 1353–1361, http://dx.doi.org/10.1366/12-06679.
[21] N.C. Dingari, I. Barman, A.K. Myakalwar, S.P. Tewari, M. Kumar Gundawar, Incorporation of support vector machines in the LIBS toolbox for sensitive and robust classification amidst unexpected sample and system variability, Anal. Chem. 84 (2012) 2686–2694, http://dx.doi.org/10.1021/ac202755e.
[22] K.-Q. Yu, Y.-R. Zhao, F. Liu, Y. He, Laser-induced breakdown spectroscopy coupled with multivariate chemometrics for variety discrimination of soil, Sci. Rep. 6 (2016), 27574, http://dx.doi.org/10.1038/srep27574.
[23] J.L. Gottfried, R.S. Harmon, F.C. De Lucia, A.W. Miziolek, Multivariate analysis of laser-induced breakdown spectroscopy chemical signatures for geomaterial classification, Spectrochim. Acta Part B At. Spectrosc. 64 (2009) 1009–1019, http://dx.doi.org/10.1016/J.SAB.2009.07.005.
[24] X. Zhu, T. Xu, Q. Lin, L. Liang, G. Niu, H. Lai, M. Xu, X. Wang, H. Li, Y. Duan, Advanced statistical analysis of laser-induced breakdown spectroscopy data to discriminate sedimentary rocks based on Czerny–Turner and Echelle spectrometers, Spectrochim. Acta Part B At. Spectrosc. 93 (2014) 8–13, http://dx.doi.org/10.1016/J.SAB.2014.01.001.
[25] M.Z. Martin, N. Labbé, T.G. Rials, S.D. Wullschleger, Analysis of preservative-treated wood by multivariate analysis of laser-induced breakdown spectroscopy spectra, Spectrochim. Acta Part B At. Spectrosc. 60 (2005) 1179–1185, http://dx.doi.org/10.1016/J.SAB.2005.05.022.
[26] J.-B. Sirven, B. Bousquet, L. Canioni, L. Sarger, S. Tellier, M. Potin-Gautier, I. Le Hecho, Qualitative and quantitative investigation of chromium-polluted soils by laser-induced breakdown spectroscopy combined with neural networks analysis, Anal. Bioanal. Chem. 385 (2006) 256–262, http://dx.doi.org/10.1007/s00216-006-0322-8.
[27] K. Bardarov, I. Buchvarov, T. Yordanova, P. Georgiev, Laser-induced break down spectroscopy for quantitative analysis of electrolytes (Na, K, Ca, Mg) in human blood serum, in: A.A. Dreischuh, D.N. Neshev, I. Staude, T. Spassov (Eds.), Int. Conf. Quantum, Nonlinear, Nanophotonics, ICQNN 2019), SPIE, 2019, 2019, p. 7, http://dx.doi.org/10.1117/12.2552209.
[28] I. Ahmed, R. Ahmed, J. Yang, A.W.L. Law, Y. Zhang, C. Lau, Elemental analysis of the thyroid by laser induced breakdown spectroscopy, Biomed. Opt. Express 8 (2017), http://dx.doi.org/10.1364/BOE.8.004865.
[29] L. Jorhem, J. Engman, B.-M. Arvidsson, B. Åsman, C. Åstrand, K.O. Gjerstad, J. Haugsnes, V. Heldal, K. Holm, A.M. Jensen, M. Johansson, L. Jonsson, H. Liukkonen-Lilja, E. Niemi, C. Thorn, K. Utterström, E.-R. Venäläinen, T. Waaler, Determination of Lead, Cadmium, Zinc, Copper, and Iron in Foods by Atomic Absorption Spectrometry after Microwave Digestion: NMKL 1 Collaborative Study, (n.d.). https://pdfs.semanticscholar.org/fb20/a37339984b416748d07ca1818657c8219d11.pdf (accessed April 20, 2018).
[30] S. Gupta, U. Khastgir, Drug information update, Lithium and chronic kidney disease: Debates and dilemmas, BJPsych Bull. 41 (2017) 216–220, http://dx.doi.org/10.1192/pb.bp.116.054031.